

Conference paper

Anton L. Maximov*, Irina A. Sizova and Salambek N. Khadzhiev

Catalysis in a dispersion medium for the hydrogenation of aromatics and hydrodearomatization in oil refining

DOI 10.1515/pac-2016-1202

Abstract: A comparative study of nickel-tungsten sulfide catalysts for hydrodearomatization prepared *in situ* in a reaction medium by different methods (from a $[\text{BMPip}]_2\text{Ni}(\text{WS}_4)_2$ precursor in a hydrocarbon or in an ionic liquid, from a suspension of nickel and tungsten salts formed from inverted emulsions in hydrocarbons, or from oil-soluble precursors) has been carried out. It has been found that the use of the oil-soluble precursors makes it possible to reach a high degree of sulfidizing of the active phase and a high degree of its promotion by nickel at a small size of the active phase particles. The resulting catalyst can be applied to the hydrogenation of both the naphthalene and substituted methylnaphthalenes (2-methylnaphthalene, 2,6-dimethylnaphthalene, 2,3-dimethylnaphthalene, and 2,3,6-trimethylnaphthalene) with the high selectivity for decalins and to the hydrodearomatization of light cycle oil with the complete removal of di- and polycyclic aromatic compounds.

Keywords: hydrodearomatization, hydrodesulfurization, nickel-tungsten sulfides, unsupported catalysts, *in situ* activation, Mendelev XX.

Introduction

The fluid catalytic cracking (FCC) process represents an integral part of a refinery complex, providing the majority of gasoline consumed throughout the world in addition to other important transportation fuels. The light cycle oil (LCO) is a by-product of this process and accounts for approximately 10–20 wt. % of FCC products [1, 2]. LCO properties like low cetane number as well as the high sulphur and nitrogen (depending on the feedstock of FCC), aromatic content, make LCO difficult to treat and use as a diesel blending component. For example, straight run gas oils usually contain 25–30 % of total aromatics, whereas LCO contains 50–75 % of total aromatics [3, 4]. The diaromatics, largely alkyl-substituted naphthalenes, are the main components of LCO [5].

The method of using the LCO without upgrading is a blend-stock into heavy fuel oil for viscosity adjustment. High pressure hydrocracking into naphtha and lighter products or severe hydrotreating of mixture of LCO with straight run diesel feed are used for LCO processing [6, 7]. As well, LCO upgrading by hydrotreating units under mild conditions is used to produce the feed of FCC units [2]. The high levels of aromatics in LCO

Article note: A collection of invited papers based on presentations at the XX Mendelev Congress on General and Applied Chemistry (Mendelev XX), held in Ekaterinburg, Russia, September 25–30 2016.

***Corresponding author: Anton L. Maximov**, A.V. Topchiev Institute of Petrochemical Synthesis, Russian Academy of Sciences, Leninskii pr. 29, Moscow 119991, Russia; and Faculty of Chemistry, Moscow State University, Moscow 119991, Russia, e-mail: max@ips.ac.ru

Irina A. Sizova and Salambek N. Khadzhiev: A.V. Topchiev Institute of Petrochemical Synthesis, Russian Academy of Sciences, Leninskii pr. 29, Moscow 119991, Russia

make it suitable to be converted into high-value aromatics feedstocks – specifically, benzene, toluene and xylenes [8], but this process is quite expensive. For all these processes, catalytic hydrogenation of diaromatics is the primary reaction that reduces the aromatic content, and it occurs before hydrocracking and isomerization [9, 10]. The traditional hydrotreating catalysts demonstrate the low activity in hydrodearomatization (hydrogenation of di- and polycyclic compounds) and even the addition of 10–30 % of LCO to diesel feed leads to decreases in the feed reactivity and requires an increase in the reactor temperature in order to meet the product sulfur target.

LCO typically contains a significant amount of sulfur (3000–25 000 ppm) and sulfur tolerant catalysts should be used for hydrogenation. Among a variety of such hydrogenation systems, Co, Mo, Ni and W as the active metal components and the $\gamma\text{-Al}_2\text{O}_3$ as support have been widely explored in the chemical industry field of petroleum and coal [3, 11–13]. The most important characteristic of NiW phase is greater hydrogenation properties than the other active phases (NiMo or CoMo) have [4, 11, 14–16].

Using of unsupported catalysts is one of the ways to increase the hydrogenation activity of systems. So the new unsupported multi-metal bulky catalyst developed by Akzo-Nobel showed ultra-high hydrodesulfurization and hydrodenitrogenation activity compared to traditional supported catalyst, representing a promising research direction in hydrotreating catalyst development [17]. Unlike the quite well documented Co(Ni)–Mo [18, 19] and Co(Ni)–Mo–W sulfide systems [20, 21], unsupported Ni–W–S catalysts have been examined to a lesser extent. As well, a few studies of unsupported NiW catalysts focus on their behavior in the hydrodesulfurization [19, 22–24] and hydroconversion of the heavy feedstock [24–27]. The activity of unsupported Ni-promoted tungsten unsupported catalysts in hydrogenation processes have been studied less, only information about hydrogenation of biphenyl [28] and toluene [29] has been presented. In the works [28, 30] a comparison of the catalytic properties of unsupported binary sulfides demonstrated that the NiW system has the best hydrogenating properties.

An alternative to bulky catalysts are systems with nanosized particles dispersed in the reaction phase. The production of catalytically active nanosized particles directly in a hydrocarbon raw material (*in situ*) with the formation of highly dispersed stable catalysts for hydroconversion and hydrogenation with the high sulfur contents of final sulfide materials (with particle sizes from 50 to 500 nm) is a new promising method for the preparation of unsupported sulfide catalysts for hydroconversion of heavy feedstocks [31–33]. Here, we report the results of a comparison of different approaches to the synthesis *in situ* of unsupported catalysts for the hydrogenation of aromatic compounds. The activities of the *in situ* prepared NiWS catalysts were compared using the hydrogenation reactions of the model compounds (naphthalene and mono-, di-, and trimethyl-substituted naphthalenes) and the hydroprocessing of LCO.

Experimental

Catalyst preparation

The formation of Ni–W–S catalysts occurred directly in the course of a catalytic reaction under the process conditions. The unsupported catalytic systems were prepared by the following methods:

- (i) the *in situ* decomposition of the precursor 1-butyl-1-methylpiperidinium nickel–thiotungsten complex $[\text{BMPip}]_2\text{Ni}(\text{WS}_4)_2$ directly in a hydrocarbon raw material [34];
- (ii) the *in situ* decomposition of the precursor $[\text{BMPip}]_2\text{Ni}(\text{WS}_4)_2$ in the ionic liquid 1-butyl-1-methylpiperidinium trifluoromethanesulfonate $[\text{BMPip}^+][\text{CF}_3\text{COO}^-]$. The required amount of the precursor was dissolved in 1 mL of the ionic liquid. The volume ratio of the hydrocarbon raw material to the ionic liquid was 1:1. As an additional source of nickel, $\text{Ni}(\text{NO}_3)_2 \cdot 6\text{H}_2\text{O}$ was introduced; it was dissolved in the ionic liquid and mixed with a solution of the precursor $[\text{BMPip}]_2\text{Ni}(\text{WS}_4)_2$ in the ionic liquid. The W:Ni molar ratio was 1:1 [35]. The ionic liquid is not mixed with the hydrocarbons and the two phases exist: the bottom phase (ionic liquid and precursors) and the top phase (hydrocarbons). Precursors are decomposed during cata-

lytic test to form NiW catalyst evenly distributed in ionic liquid. The reaction products can be separated by simple decantation for the reuse of the catalyst.

- (iii) the *in situ* decomposition of a suspension of the solid particles of the precursor $\text{Ni}/(\text{NH}_4)_2\text{WS}_4$ in a hydrocarbon raw material stabilized with the surfactant Span 80. The suspensions of the $\text{Ni}/(\text{NH}_4)_2\text{WS}_4$ solid particles in the hydrocarbon raw material were obtained by the distillation of water from mixed inverted emulsions based on the aqueous solutions of $(\text{NH}_4)_2\text{WS}_4$ and $\text{Ni}(\text{NO}_3)_2 \cdot 6\text{H}_2\text{O}$ in the hydrocarbon raw material stabilized with 5.0 wt. % Span 80. The W:Ni molar ratio was 1:1 [36];
- (iv) the *in situ* decomposition of oil-soluble precursors (tungsten hexacarbonyl and nickel(II) 2-ethylhexanoate) in a hydrocarbon raw material. The salts were dissolved in the hydrocarbon raw material; 2.5 wt. % of elemental sulfur was added to the hydrocarbon raw material as a sulfidizing agent for the formation of metal sulfides, which are active in the hydrogenation reactions of the aromatic hydrocarbons. The W:Ni molar ratio was 1:2 [37].

The prepared catalysts were labeled as NiWS-*hc*, NiWS-*IL*, NiWS-*wsp* and NiWS-*osp*, respectively.

For the reference, the activity data for an industrial hydrogenation catalyst NiWS-A produced at the Angarsk factory of catalysts and organic synthesis have also been shown. It consists of nickel and tungsten sulfides and active alumina (Ni 16.0 wt. %; WO_3 30.6 wt. %; S 17.5 wt. %; specific surface area – 103 m^2/g).

Catalyst characterization

The textural characteristics of catalysts were determined by low-temperature nitrogen adsorption by means of a Micromeritics ASAP 2020 instrument. The parameters were calculated by the Brunauer–Emmett–Teller (BET) method using the dedicated software. X-ray diffraction (XRD) analysis of the samples was carried out using a Rigaku D/Max-RC diffractometer (12 kW X-ray source, Cu rotating anode, flat graphite analyzer crystal, scintillation counter). The structure and morphology of the *in situ* prepared catalyst samples were studied by a JEM-2100 analytical electron microscope from JEOL. The average length of particles and the number of layers in multilayer agglomerates were determined by the statistical estimation of the dimensional characteristics of more than 300 active component particles in different TEM images. The samples were analyzed by X-ray photoelectron spectroscopy (XPS) using a PHI-5500 ESCA X-ray photoelectron spectrometer from physical Electronics. Nonmonochromatic Al K α radiation ($h\nu = 1486.6$ eV) with the power of 300 W used for the excitation of photoemission. Powders were pressed into an indium plate. The analysis zone diameter was 1.1 mm. The calibration of photoelectron peaks was based on the C 1s line with a binding energy of 284.9 eV. The deconvolution of spectra was carried out by a nonlinear least squares method with the use of Gaussian and Lorentzian functions.

Catalytic tests

The catalytic hydrogenation experiments were carried out in a steel autoclave at the initial hydrogen pressure of 5.0 MPa and the temperature of 350 °C for 10 h. The 10 wt. % solutions of aromatic compounds (naphthalene, 2-methylnaphthalene, 2,3-dimethylnaphthalene, 2,6-dimethylnaphthalene, and 2,3,6-trimethylnaphthalene) in *n*-hexadecane were tested as model substances. The aromatic compound to W molar ratio was 105:1. The hydrogenation products of the model systems were analyzed by means of the Kristallyuks 4000 M chromatograph equipped with a flame-ionization detector and an SPB[®]-1 capillary column (30 m \times 0.25 mm) with a polydimethylsiloxane stationary liquid phase; helium was used as a carrier gas, and a split ratio was 1:90. The chromatograms were treated with the use of the NetChromWin software.

The LCO hydrofining products were analyzed for the total sulfur content with the aid of an EA 3100 instrument with a UV detector. The degree of hydrodesulfurization (HDS, %) was evaluated based on the conversion of the total sulfur. The aromatic hydrocarbon content was determined by HPLC according to the GOST [State

Table 1: Specific surface areas.

	NiWS- <i>hc</i>	NiWS- <i>IL</i>	NiWS- <i>wsp</i>	NiWS- <i>osp</i>
Specific surface areas, m ² /g	33.6	30.2	25.3	41.2

Standard] R EN 12916-08 by means of a Knauer analytical instrument with a Smartline 2300 refractometric detector (the mobile phase *n*-heptane; the column Diasfer 80 amine; and the analysis temperature 20 °C).

Results and discussion

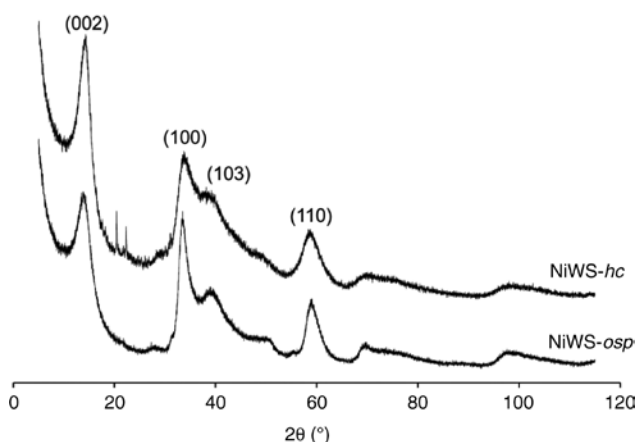
Physicochemical characteristics of the *in situ* prepared Ni–W–S particles

The use of different precursors led to essential differences in the morphology, size, and characteristics of the active phase formed in the course of a catalytic reaction.

Specific surface areas for all catalysts are reported in Table 1. Surface areas for the *in situ* obtained catalysts were measured after the hydrogenation reaction. The results of nitrogen adsorption isotherm for NiWS-*osp* show the highest surface area (51.2 m²/g). The variation of surface areas of WS₂ catalysts can be in the range of a few to several 100 m²/g depending on the precursor and condition of the synthesis [38–40]. However, for lamellar sulfides the overall surface area does not directly correlate with the activity.

XRD patterns for the unsupported NiW sulfides are presented in Fig. 1. All of the patterns are in agreement with those reported for poorly crystalline WS₂ structures [41, 42]. The presence of the (002) peak at $2\theta \approx 14^\circ$ is representative for the stacking slabs along the *c*-axis, while the presence of the (110) peak at $2\theta \approx 59^\circ$ is representative of a slab layer. The XRD patterns for all catalysts are quite similar whatever the type of precursors. The NiWS-*IL* catalyst (not shown here) shows poorer crystalline structure than NiWS catalysts formed from other precursors. The sharp peaks ($2\theta \approx 23^\circ$) due to a complex distribution of nickel sulfide phase Ni₉S₈ are detected for the NiWS-*hc* catalyst and NiWS-*wsp*. In addition, Ni₃S₂ phase with weak diffraction peaks at $2\theta \approx 30^\circ$, 45° and 54° presents in NiWS-*wsp* and NiWS-*IL* catalysts. For NiWS-*osp*, XRD patterns did not present peaks of Ni phases, suggesting that promoter atoms are well dispersed on the active phase.

The representative TEM micrographs of four catalysts are shown in Fig. 2. All of the catalysts were characterized by a typical lamellar phase structure as WS₂ nanoplates combined in agglomerates. The interplanar spacing of 6.57 Å is indicative of the (002) basal plane of a crystalline WS₂ [43]. The TEM data allowed us

**Fig. 1:** XRD patterns for NiWS catalysts.

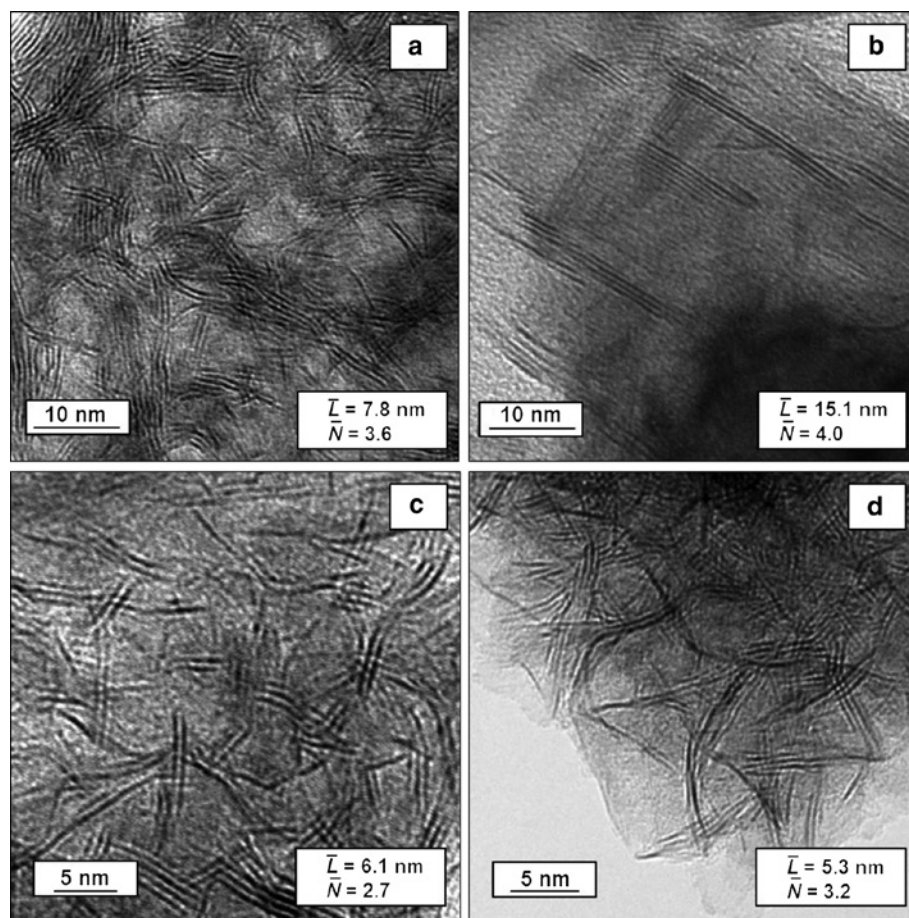


Fig. 2: Micrographs of the Ni–W–S catalysts prepared by the *in situ* decomposition of the precursors. (a) NiWS-*hc*, (b) NiWS-*IL*, (c) NiWS-*wsp*, and (d) NiWS-*osp*.

to calculate the average dimension of the NiWS phase particles, which varied from 5.3 to 15.1 nm, and the average stacking number in the WS₂ crystallites varied from 2.7 to 4.0.

NiWS-*IL* catalyst obtained in the ionic liquid had larger average length of the NiWS particles compared to the NiWS-*hc* catalyst obtained by the decomposition of the same precursor. The concentration of the particles with the lengths greater than 20 nm in the catalyst NiWS-*hc* was no higher than 5 wt. %, whereas the fraction of such particles was greater than 30 wt. % in the catalyst NiWS-*IL*. The average length of NiWS particles was the smallest for NiWS-*osp* catalyst (5.3 nm). The smallest average number of layers was for a catalyst NiWS-*wsp* (2.7); this number was as high as 3.2 for NiWS-*osp*. The average number of layers in the multilayered agglomerate for the catalyst NiWS-*hc* (3.6) was also somewhat lower than that for the catalyst obtained in the ionic liquid (4.0). The experimental data indicated that the use of a surfactant in the NiWS catalyst preparation leads to the formation of particles with a smaller number of layers in the multilayered agglomerate but with a wide layer-length distribution.

One should note that the degree of agglomeration of multilayered catalyst particles in a reaction medium also depends on the method of synthesis. In the general case, the *in situ* preparation of NiWS particles in hydrocarbon raw materials leads to the formation of the shorter sulfide nanoparticles located closely to each other in the agglomerates. The smallest size of agglomerates (100–200 nm) was typical for the catalyst NiWS-*osp*, and a maximum size (to 1 μm) was typical for the catalyst NiWS-*hc*. On the contrary, in the synthesis of particles in the ionic liquid (catalyst NiWS-*IL*), larger nanoplates were located far from each other, and they were almost non-agglomerated. The decomposition of a precursor in the ionic liquid is likely to occur through associates dissolved precursor and leads to a considerable lengthening of the Ni–W–S particles without their agglomeration.

The XPS data make it possible to characterize the electronic states of metals in the active phase of a catalyst (Table 2) [27] and to estimate the degree of its promotion with nickel. The maximum tungsten content of the sulfide form was for the catalyst NiWS-*osp* (67 %), and the smallest content was for the catalyst NiWS-*IL* (only 26.4 % tungsten occurred in the form of the sulfide on the surface). A comparatively low degree of sulfidizing of the catalyst surface obtained in the ionic liquid was confirmed by the data on the deconvolution of the S 2*p* level [44, 45]. On the surface of NiWS-*IL* catalyst, sulfur mainly occurred in the form of an oxy-sulfide (63.4 %) or in the form of a sulfide (65 %) upon the decomposition of the same precursor in hydrocarbon raw materials. For the other two catalysts, the fraction of sulfur in the sulfide form was 42–45 %.

As a rule, the activity of the test catalysts in hydroprocesses depends on the concentration of a mixed Ni–W–S phase, which characterizes the degree of promotion with nickel. Figure 3 shows the examples of decomposition of Ni 2*p* photoelectron spectra recorded for NiWS-*osp* catalyst. The XPS data are indicative for the presence of nickel in the following three states: as the sulfide NiS_x (Ni₂S₃, Ni₉S₈, NiS), a Ni–W–S phase (the signals at 853.7 ± 0.2 eV is related 2*p*_{3/2} level; 870.9 ± 0.2 eV is related Ni 2*p*_{1/2} level), and the NiO species, in which nickel is bound to oxygen [46, 47]. The peaks that are not marked in color correspond to the satellites.

On the surface of the NiWS-*IL* catalyst, the sulfide nickel content was no higher than 7 % and a considerable fraction of this metal (70 %) occurred in an oxygen environment. In the catalyst NiWS-*hc* about 60 % nickel occurred in a sulfide environment and 40 % nickel constituted a complex Ni–W–S sulfide. For catalyst NiWS-*wsp* almost a third of nickel occurred in the sulfide form and only 15.5 % accounted for a promoted phase. A maximum concentration of the Ni–W–S phase with the almost complete absence of NiS_x was for the catalyst NiWS-*osp*.

Table 2: XPS data for the W 4*f*, Ni 2*p*, and S 2*p* levels.

Element	Fraction (rel. %)				State
	NiWS- <i>hc</i>	NiWS- <i>IL</i>	NiWS- <i>wsp</i>	NiWS- <i>osp</i>	
W4 <i>f</i>	61.7	26.4	56.3	67.2	WS ₂
	8.1	30.1	16.0	11.9	WO _x S _y
	30.2	43.5	27.7	20.9	WO ₃
Ni2 <i>p</i>	17.8	7.1	27.0	1.9	NiS
	41.1	23.0	15.5	67.0	Ni–W–S
	41.1	69.9	57.5	31.1	NiO
S2 <i>p</i>	64.9	36.6	42.9	45.5	S ²⁻
	30.2	63.4	38.9	47.8	S ₂ ²⁻
	4.9	–	18.1	6.7	(SO ₄) ²⁻

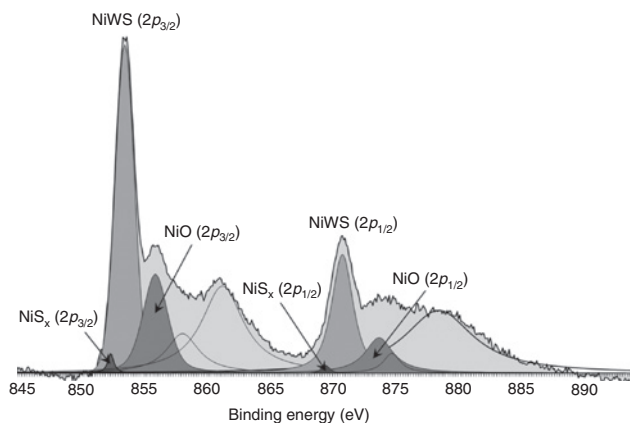


Fig. 3: XPS Ni 2*p* spectrum of NiWS-*osp* catalyst.

The difference in the structures of the phases obtained is likely to depend on difference between the mechanisms of catalyst formation and sulfidizing. With the use of $[\text{BMPip}]_2\text{Ni}(\text{WS}_4)_2$ in a hydrocarbon medium as a precursor, the particle size of agglomerated sulfide depends on the particle size of the suspended precursor; the length and the number of sulfide layers depend on the rate of sulfide decomposition. And the degree of promotion depends on the presence of nickel bound to sulfur atoms in the starting compound. In the ionic liquid, the formation of sulfide from a solution of the specified precursor occurred, and the length of sulfide layers distributed in the polar solvent had increased instead of the agglomeration; the presence of oxygen in a counterion led to an increase in the fraction of an oxide phase. In the suspension synthesis, the size of the sulfide particle agglomerates depended on the particle size of tungsten oxide in the suspension and on the rate of its sulfidizing. In this case, promotion with nickel was minimal: nickel oxide was mainly converted into sulfide. The rate of the reactions of oil-soluble precursors with sulfur was responsible for the size of catalyst particle aggregates and for the high fraction and the morphology of lamellar sulfide particles, while the presence of nickel ions in the form of monomolecular particles ensured the formation of a high fraction of the promoted phase.

Hydrogenation of model substrates

A comparison of the catalytic activities of the NiWS particles, obtained by the decomposition of different precursors, based on an example of the reaction of naphthalene hydrogenation with tetralins and decalins formation, showed that the conversion of naphthalene was as high as 92–100 % for 10 h with the use of all of the test systems (Fig. 4). The activity of an industrial hydrogenation catalyst NiWS-A was higher than NiWS-IL and NiWS-wsp and significantly lower than NiWS-hc and NiWS-osp, especially in decalin formation. The use of NiWS-osp led to the exhaustive formation of decalins; *trans*-decalin, which is thermodynamically more stable, was the main reaction product and the ratio between *cis*- and *trans*-decalins was 1:2.6. The low yields of decalins were observed upon NiWS-IL and NiWS-wsp. These two systems exhibited a low Ni fraction in the Ni–W–S complex sulfide (Table 2) [48, 49]. This is most likely to be due to using water and an oxygen-containing surfactant for the stabilization of particles during the obtaining of the catalyst NiWS-wsp. The replacement of water by a sulfur-containing polar solvent and an increase in the reaction temperature can lead to an increase in the activity of the resulting particles due to additional surface sulfidizing. Thus, the use of dimethyl sulfoxide (DMSO) in place of water and an increase in the process temperature to 380 °C leads to an increase in the yield of decalins to 82 % with the exhaustive hydrogenation of naphthalene.

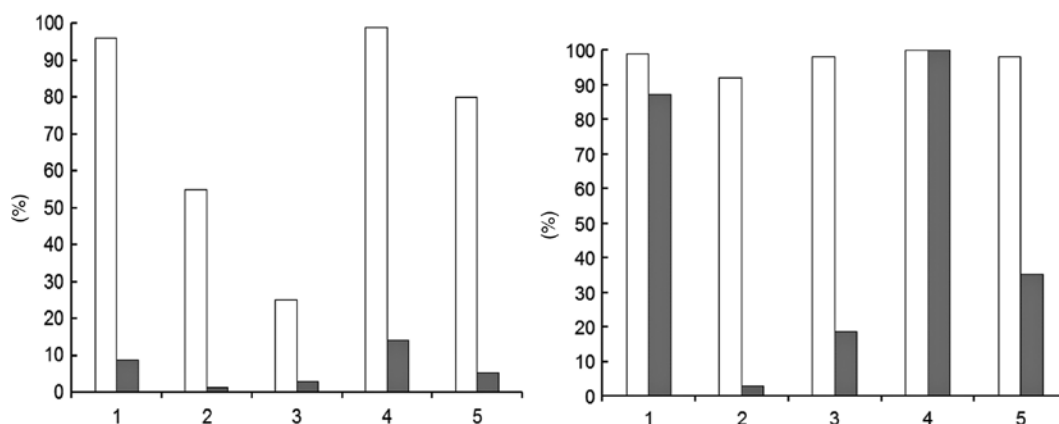
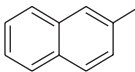
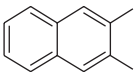
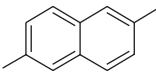
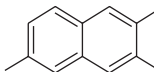
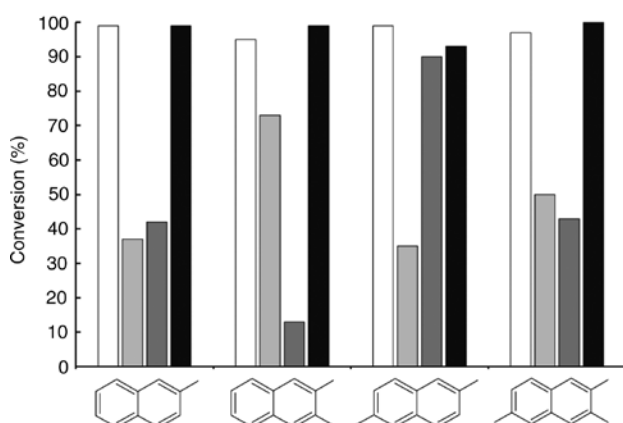


Fig. 4: Dependence of (white columns) the conversion of naphthalene and (gray columns) the yield of decalins on the catalysts used: (1) NiWS-hc, (2) NiWS-IL, (3) NiWS-wsp, (4) NiWS-osp and (5) NiWS-A. Reaction conditions: 350 °C, 5.0 MPa, 3 h (left) and 10 h (right).

Table 3: Dependence of the yield of decalins on the precursor used.

Catalyst				
NiWS- <i>hc</i>	23	5	46	8
NiWS- <i>IL</i>	1	4	0,4	2
NiWS- <i>wsp</i>	0	0	2	0
NiWS- <i>osp</i>	92	40	56	55

Reaction conditions: 350 °C, 5.0 MPa, and 10 h.

**Fig. 5:** Conversion of naphthalenes with the use of the following catalysts: (white columns) NiWS-*hc*, (light grey columns) NiWS-*IL*, (dark grey columns) NiWS-*wsp* I, and (black columns) NiWS-*osp*. Reaction conditions: 350 °C, 5.0 MPa, and 10 h.

Not only a catalyst preparation method but also different steric peculiarities of a substrate effect the reaction rate of the aromatic compounds hydrogenation. The presence of the electron-donor substituents facilitates the occurrence of a hydrogenation reaction of a conjugated aromatic system because of an increase in the electron density and an increase in the degree of substrate adsorption on the surface of an active phase [15]. At the same time, the presence of these substituents can prevent a molecular orientation favorable for hydrogenation on the sulfide surface. From naphthalene to 2-methylnaphthalene (the inclusion of a methyl substituent at an aromatic ring of naphthalene), the yield of decalins decreased (Table 3) with the retention of a high conversion (Fig. 5) with the use of even the most active catalyst NiWS-*osp*. For reaction in hydrocarbon media the introduction of the second methyl substituent into the same aromatic ring (2,3-dimethylnaphthalene) led to a sharp decrease in the conversion, whereas, on the contrary, the appearance of a substituent at the second ring (2,6-dimethylnaphthalene) led to an increase in the conversion. For NiWS-*IL* catalyst, in addition to different substrate solubilities in the ionic liquid, the specific solvation interactions between the π -system of an aromatic compound and the bulky cation of the ionic liquid exert a considerable effect, which can lead to higher conversion of substrate with second methyl substituent at the second ring (2,6-dimethylnaphthalene). The presence of one or more methyl substituents in an aromatic ring decreased the yield of decalins due to the steric hindrances too.

For all of the test aromatic compounds, the highest rates of hydrogenation and selectivity for decalins were observed with the use of a catalyst NiWS-*osp*. This was most likely due to the high fraction of Ni in the Ni–W–S phase (67 %), the high dispersity of active phase particles, and the smallest size of the agglomerates of sulfide particles in solution. Even with the use of 2,3,6-trimethylnaphthalene as the most sterically hindered substrate, the yield of decalins was 55 %. A low yield of decalins (8 %) was observed within a catalyst with a much larger size of agglomerates (NiWS-*hc*).

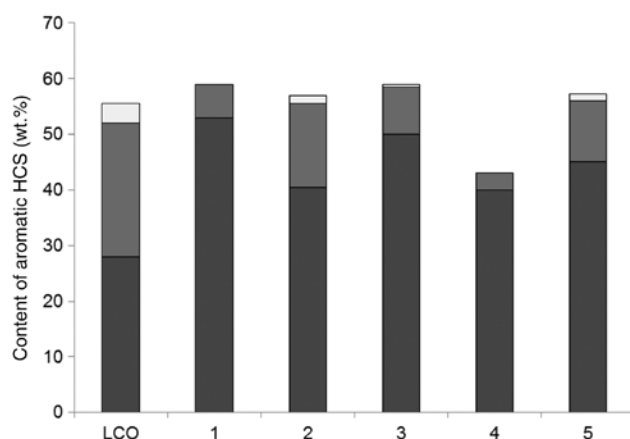


Fig. 6: Concentrations of (dark gray columns) MAHs, (light gray columns) BAHs, and (white columns) PAHs in LCO and hydrogenates depending on the catalysts used: (1) NiWS-*hc*, (2) NiWS-*IL*, (3) NiWS-*wsp*, (4) NiWS-*osp*, (5) NiWS-A. Reaction conditions: 350 °C, 5.0 MPa, and 10 h.

Hydrogenation and hydrodesulfurization of LCO

The catalytic activity of NiWS particles prepared by the different methods in the hydrotreating reaction of LCO was compared at a 2 wt. % tungsten content of the raw material (Fig. 6).

The hydrodearomatization of LCO is similar to the hydrogenation of model substances. Thus, for all of the test catalytic systems, the concentration of monocyclic aromatic hydrocarbons (MAHs) increased with the degree of hydrodearomatization of bicyclic aromatic hydrocarbons (BAHs) and polycyclic aromatic hydrocarbons (PAHs); this was related to the formation of both naphthenic and MAHs upon the hydrogenation of BAHs and PAHs.

The exhaustive hydrogenation of PAHs was observed with the use of the catalysts NiWS-*hc* obtained directly in the hydrocarbon raw material (in LCO) and on NiWS-*osp*, which had the highest fractions of Ni in the composition of a Ni–W–S phase (see Table 1). The use of a catalyst NiWS-*hc* also led to a significant decrease in the BAH content (by a factor of >4); however, a notable increase in the MAH content was observed to indicate only the partial hydrogenation of compounds containing two or more aromatic rings with the formation of MAHs. The use of a catalyst NiWS-*osp* led to the highest degree of LCO hydrodearomatization and the degree of hydrodesulfurization (HDS = 96.3 %) (Table 4); this fact allowed us to consider this system as an optimum for the *in situ* formation of NiWS catalysts in a hydrocarbon medium.

In this way, NiWS-*IL* catalyst shows the worst activity in both hydrodearomatization and hydrodesulfurization reactions. This catalyst was characterized by the largest average length of the sulfide particles (15.1 nm), the largest number of the layers and the low Ni content in the NiWS phase. If the “rim-edge” model proposed by Daage and Chianelli [50] for MoS₂ particles has been considered, sulfur hydrogenolysis would take place on both rim and edge sites, while hydrogenation occurs only on the “rim” sites. The large average length of the sulfide particles leads to the decreasing of W edge sites, and the large number of layers leads to

Table 4: The sulfur content in the hydrogenation product.

Catalyst	Sulfur content (ppm)	HDS (%)
NiWS- <i>hc</i>	187	94.6
NiWS- <i>IL</i>	545	84.0
NiWS- <i>wsp</i>	145	95.8
NiWS- <i>osp</i>	131	96.3
NiWS-A	320	90.8

the decreasing of the W rim sites, that in general leads to the low activity in the both processes. The hydrodesulfurization activity of the NiWS-*wsp* catalyst is higher than for NiWS-*hc* and NiWS-*IL* catalysts due to the smaller average length and the number of layers that leads to the increasing of both the rim and edge sites. The NiWS-*osp* catalyst is the most active in both the hydrodearomatization and hydrodesulfurization reactions owing to the smallest average length and the highest Ni content in the NiWS phase.

Conclusions

In summary, we have compared the composition and catalytic activity of NiWS particles obtained by the *in situ* decomposition of the different precursors. We have found that the precursor and the method of its introduction into the catalytic system exert the essential effect on the structure peculiarities of the *in situ* formed tungsten-containing sulfide catalyst. Oil-soluble tungsten hexacarbonyl and nickel (II) 2-ethylhexanoate are optimum precursors for the *in situ* formation of a Ni–W sulfide catalyst highly active in the hydrogenation reactions of aromatic hydrocarbons. The use of this catalyst makes it possible to reach the high conversions of the model substances, the high selectivity for decalins, and the high degrees of LCO dearomatization.

Acknowledgments: This work has been supported by the Russian Science Foundation, the agreement no. 15-13-00123.

References

- [1] V. P. Thakkar, S. F. Abdo, V. A. Gembicki, J. F. Mc Gehee, UOP Report AM-05-53 (2005).
- [2] C. Peng, X. Fang, R. Zeng, R. Guo, W. Hao. *Catal. Today*. **276**, 11 (2016).
- [3] H. Toulhoat, P. Raybaud. *Catalysis by Transition Metal Sulphides*. – P.: Editions Technip, p. 787, (2013).
- [4] A. Stanislaus, A. Marafi, M. S. Rana. *Catal. Today* **153**, 1 (2010).
- [5] V. Sugumaran, H. Biswas, A. Yadav, J. Christopher, V. Kagdiyal, M. B. Patel, B. Basu. *Energy Fuels*. **29**, 2940 (2015).
- [6] C. G. Laredo, R. Saint-Martin, C. M. Martinez, J. Castillo, L. J. Cano. *Fuel*. **83**, 1381 (2004).
- [7] Z. Dukanovic, S. B. Glisic, V. J. Cobanin, M. Niciforovic, C. A. Georgiou, A. M. Orlovic. *Fuel Process. Tech.* **106**, 160 (2013).
- [8] S. J. Kim, S. C. Kim, J. Kawasaki. *Sep. Sci. Technol.* **38**, 179 (2003).
- [9] Y. Zhao, B. J. Shen, W. C. Zhang, R. Tian, Z. H. Zhang, J. Gao. *Fuel*. **87**, 2343 (2008).
- [10] M. Gupta, J. He, T. Nguyen, F. Petzold, D. Fonseca, J. B. Jasinski, M. K. Sunkara. *Appl. Catal. B: Environ.* **180**, 246 (2016).
- [11] R. Tong., Y. Wang, X. Zhang, H. Zhang, J. Dai, X. Lin, D. Xu. *J Fuel Chem Technol.* **43**, 1461 (2015).
- [12] H. Zhang, Y. Wang, P. Zhang, X. Lin, Y. Zhu. *J Fuel Chem Technol.* **41**, 1085 (2013).
- [13] J. H. Yang, J. J. Kuang, Y. L. Chen. *Chem Eng.* **40**, 10 (2012).
- [14] T. Alphazan, A. Bonduelle-Skrzypczak, C. Legens, Z. Boudene, A.-L. Taleb, A.-S. Gay, O. Ersen, C. Coperet, P. Raybaud. *J. Catal.* **340**, 60 (2016).
- [15] A. Stanislaus, B. H. Cooper. *Catal. Rev. – Sci. Eng.* **36**, 75 (1994).
- [16] E. J. M. Hensen, Y. van der Meer, J. A. R. van Veen, J. W. Niemantsverdriet. *Appl. Catal. Gen.* **322**, 16 (2007).
- [17] L. Zhang, X. Long, D. Li, X. Gao. *Catal. Commun.* **12**, 927 (2011).
- [18] L. Yue, G. Li, F. Zhang, L. Chen, X. Li, X. Huang. *Appl. Catal. A Gen.* **512**, 85 (2016).
- [19] P. Li, Y. Chen, C. Zhang, B. Huang, X. Liu, T. Liu, Z. Jiang, C. Li. *Appl. Catal. A: Gen.* **533**, 99 (2017).
- [20] R. Huirache-Acuna, G. Alonso-Núñez, F. Paraguay-Delgado, J. Lara-Romero, G. Berhault, E. M. Rivera-Munoz. *Catal. Today*, **250**, 28 (2015).
- [21] C. Yin, H. Liu, L. Zhao, B. Liu, S. Xue, N. Shen, Y. Liu, Y. Li, C. Liu. *Catal. Today*. **259**, 405 (2016).
- [22] L. Zhang, P. Afanasiev, D. Li, X. Long, M. Vrinat. *Catal. Commun.* **8**, 2232 (2007).
- [23] L. Zhang, P. Afanasiev, D. Li, Y. Shi, M. Vrinat. *Comptes Rendus Chimie*. **11**, 130 (2008).
- [24] Y. Yi, B. Zhang, X. Jin, L. Wang, C. T. Williams, G. Xiong, D. Su, C. Liang. *J. Mol. Catal. A* **351**, 120 (2011).
- [25] Y. G. Hur, D.-W. Lee, K.-Y. Lee. *Fuel*. **185**, 794 (2016).
- [26] S. G. Jeon, J.-G. Na, C. H. Ko, K. B. Lee, N. S. Rho, S. B. Park. *Mater. Sci. Eng. B*. **176**, 606 (2011).
- [27] K. Tayeb, C. Lamonier, C. Lancelot, M. Fournier, E. Payen, A. Bonduelle, F. Bertoncini. *Catal. Today*. **150**, 207 (2010).
- [28] M. Lacroix, M. Vrinat, M. Breyse. *Appl. Catal.* **21**, 73 (1986).
- [29] L. Zhang, P. Afanasiev, D. Li, X. Long, M. Vrinat. *Catal. Today*. **130**, 24 (2008).

- [30] M. Vrinat, M. Lacroix, M. Breyse, R. Frety. *Bull. Sot. Chim. Belg.* **93**, 697 (1984).
- [31] S. N. Khadzhiev, H. M. Kadiev, M. H. Kadieva. *Petrol. Chem.* **54**, 323 (2014).
- [32] S. N. Khadzhiev. *Petrol. Chem.* **56**, 465 (2016).
- [33] K. Wilkinson, M. D. Merchan, P. T. Vasudevan. *J. Catal.* **171**, 325 (1997).
- [34] I. A. Sizova, S. I. Serdyukov, A. L. Maksimov. *Petrol. Chem.* **55**, 468 (2015).
- [35] I. A. Sizova, S. I. Serdyukov, A. L. Maksimov, N. A. Sinikova. *Petrol. Chem.* **55**, 38 (2015).
- [36] I. A. Sizova, S. I. Serdyukov, A. L. Maksimov. *Petrol. Chem.* **56**, 131 (2016).
- [37] I. A. Sizova, A. B. Kulikov, M. I. Onishchenko, S. I. Serdyukov, A. L. Maksimov. *Petrol. Chem.* **56**, 44 (2016).
- [38] J. Espino, L. Alvarez, C. Ornelas, J. L. Rico, S. Fuentes, G. Berhault, G. Alonso. *Catal. Lett.* **90**, 71 (2003).
- [39] G. Alonso, R. R. Chianelli. *J. Catal.* **221**, 657 (2004).
- [40] G. Alonso, M. Del Valle, J. Cruz, A. Licea-Claverie, V. Petranovskii, S. Fuentes. *Catal. Lett.* **52**, 55 (1998).
- [41] K. S. Liang, R. R. Chianelli, F. Z. Chien, S. C. Moss. *J. Non-Cryst. Solids.* **79**, 251 (1986).
- [42] R. Hashemi, N. N. Nassar, P. P. Almao. *Appl. Energy.* **133**, 374 (2014).
- [43] X. Jin, C. Ma, Y. Yi, Q. Zhang, J. Qiu, C. Liang. *J. Phys. Chem. Solids.* **71**, 642 (2010).
- [44] T. K. T. Ninh, D. Laurenti, E. Leclerc, M. Vrinat. *Appl. Catal. A Gen.* **487**, 210 (2014).
- [45] T. K. T. Ninh, L. Massin, D. Laurenti, M. Vrinat. *Appl. Catal. A Gen.* **407**, 29 (2011).
- [46] L. G. Woolfolk, C. Geantet, L. Massin, D. Laurenti, J. A. D. Reyes. *Appl. Catal. B Environ.* **201**, 331 (2017).
- [47] D. Ishutenko, P. Minaev, Y. Anashkin, M. Nikulshina, A. Mozhaev, K. Maslakov, P. Nikulshin. *Appl. Catal. B Environ.* **203**, 327 (2017).
- [48] R. R. Chianelli, T. A. Pecoraro, T. R. Halbert, W. H. Pan, E. I. Stiefel. *J. Catal.* **86**, 226 (1984).
- [49] A. N. Startsev. *Sulfide Hydrotreating Catalysts: Synthesis, Structure, and Properties*, Geo, Novosibirsk (2007).
- [50] M. Daage, R. R. Chianelli. *J. Catal.* **149**, 414 (1994).